Global and Self-consistent Simulation of ICRF Heating in Toroidal Plasmas

S. Murakami[1], A. Fukuyama[1], T. Akutsu[1], N. Nakajima[2], V. Chan[3], M. Choi[3], S.C. Chiu[4], L. Lao[3], V. Kasilov[5], T. Mutoh[2], R. Kumazawa[2], T. Seki[2], K. Saito[2], T. Watari[2], M. Isobe[2], T. Saida[2], M. Osakabe[2], M. Sasao[6] and LHD Experimental Group

[1]*Department of Nuclear Engineering, Kyoto University, Kyoto 606-8501, Japan*
[2]*National Institute for Fusion Science, Oroshi, Toki, Gifu 509-5292, Japan*
[3]*General Atomics, P.O. Box 85608, San Diego, California 92186-5608, USA*
[4]*Sunrise R&M, Inc., 8585 Hopseed Lane, San Diego, California 92129, USA*
[5]*Institute of Plasma Physics, National Science Center, KIPT, Kharkov, Ukraine*
[6]*Graduate School of Engineering, Tohoku University, Sendai 980-8579, Japan*

Abstract. The ICRF heating in toroidal plasmas is studied using two global simulation codes: a full wave field solver TASK/WM and a drift kinetic equation solver GNET. The codes are applied to both tokamaks and helical systems. The full wave code TASK/WM evaluates the realistic wave electric field, in which the effect of the self-consistent non-Maxwellian velocity distribution on the wave propagation is taken into account. GNET solves a linearized drift kinetic equation (5D phase-space) for energetic ions including complicated behavior of trapped particles in helical systemsCharacteristics of energetic ion distributions in the phase space are investigatedSelf-consistent analysis including the effect of energetic ion distribution on the fast wave propagation is also reported for tokamak plasmas.

Keywords: ICRF hating, global simulation, tokamak, helical, LHD
PACS: 52.25.Dg, 52.35.Mw, 52.50.Qt, 52.55.Fa, 52.55.Hc

INTRODUCTION

ICRF heating generates highly energetic trapped ions, which drift around the torus for a long time (typically on a collisional time scale) interacting with the RF wave field. Thus, the behavior of these energetic ions is strongly affected by the characteristics of the drift motions, that depend on the magnetic field configuration. In particular, in a 3D magnetic configuration, complicated drift motions of trapped particles would play an important role in the confinement of the energetic ions and the ICRF heating process.

Additionally, since the wavelength of the ICRF heating is typically comparable to the plasma scale length and the 3D geometry effect on the RF wave field would be also important in a 3D magnetic configuration. Therefore a global simulation of ICRF heating is

CP787, *Radio Frequency Power in Plasmas:16th Topical Conference on Radio Frequency Power in Plasmas*
edited by Stephen J. Wukitch and Paul T. Bonoli

necessary for the accurate modeling of the plasma heating process in a 3D magnetic configuration.

Also, the tail ion distribution changes the affects the fast wave propagation and the absorption rate. Thus, the self-consistent treatment of the wave field and the energetic ion tail distribution is necessary for the accurate evaluation of the ICRF heating.

In this paper we, first, study the ICRF heating in the LHD using two global simulation codes; a drift kinetic equation solver GNET [1, 2] and a wave field solver TASK/WM[3]. Both codes are taken into account the 3D geometry using the numerically obtained 3D MHD equilibrium. Then, we describe the development of the self-consistent ICRF heating simulation in a tokamak plasma with TASK code.

GLOBAL SIMULATION IN A 3D MAGNETIC CONFIGURATION

In order to study the ICRF heating in a 3D magnetic field configuration we have been developing a global simulation code combining two global codes; GNET and TASK/WM.

GNET solves a linearized drift kinetic equation for energetic ions including complicated behavior of trapped particles in 5-D phase space

$$\frac{\partial f}{\partial t} + (\mathbf{v}_{//} + \mathbf{v}_D)\cdot\nabla f + \mathbf{a}\cdot\nabla_{\mathbf{v}} f \; - C(f) - Q_{ICRF}(f) - L_{particle} = S_{particle} \tag{1}$$

where $C(f)$ and Q_{ICRF} are the linear Coulomb Collision operator and the ICF heating term. $S_{particle}$ is the particle source term by ionization of neutral particle and the radial profile of the source is evaluated using AURORA code

. The particle sink (loss) term, $L_{particle}$, consists of two parts; one is the loss by the charge exchange loss assuming the same neutral particle profile as the source term calculation and the other is the loss by the orbit loss escaping outside of outermost flux surface.

The Q_{ICRF} term is modeled by the Monte Carlo method. When the test particle pass through the resonance layer where $\omega - k_{//} v_{//} = n\omega_c$, the perpendicular velocity of this particle, $\mathrm{v}_{\perp 0}$, is changed by the following amount

$$\begin{aligned}\Delta \mathrm{v}_\perp &= \sqrt{\left(\mathrm{v}_{\perp 0} + \frac{q}{2m} I|E_+| J_{n-1}(k_\perp \rho)\,\cos\phi_r\right)^2 + \frac{q^2}{4m^2}\left\{I|E_+| J_{n-1}(k_\perp\rho)\right\}^2\,\sin^2\phi_r} - \mathrm{v}_{\perp 0} \\ &\approx \frac{q}{2m} I|E_+| J_{n-1}(k_\perp\rho)\,\cos\phi_r + \frac{q^2}{8m^2 \mathrm{v}_{\perp 0}}\left\{I|E_+| J_{n-1}(k_\perp\rho)\right\}^2\,\sin^2\phi_r\end{aligned} \tag{2}$$

where E_+ and ϕ_r are the RF wave electric fields and random phase, respectively. Also, q, m, ρ, J_n are the charge, mass and the Larmor radius of the particle, and n-th Bessel function, respectively. The time duration passing through the resonance layer, I, is given by the minimum value as, $I = \min(\sqrt{2\pi / n\dot{\omega}}\,,\, 2\pi(n\ddot{\omega}/2)^{-1/3} Ai(0))$, which corresponds to two

cases; the simply passing of the resonance layer and the passing near the turning point of a trapped motion (banana tip).

The spatial profile of RF wave electric field is necessary for the accurate calculation of the ICRF heating. The profile of RF wave field is an important factor on the ICRF heating and these profiles affect the particle orbit. We evaluate the RF wave field by the TASK/WM code. TASK/WM solves Maxwell's equation for RF wave electric field, $\mathbf{E}_{RF}$, with complex frequency, ω, as a boundary value problem in the 3D magnetic configuration.

$$\nabla \times \nabla \times \mathbf{E}_{RF} = \frac{\omega^2}{c^2} \vec{\varepsilon} \cdot \mathbf{E}_{RF} + i\omega\mu_0 \mathbf{j}_{ext}, \tag{3}$$

Here, the external current, $\mathbf{j}_{ext}$, denotes the antenna current in ICRF heating. The response of the plasma is described by a dielectric tensor including kinetic effects in a local normalized orthogonal coordinates.

We apply the global simulation code to a LHD configuration (R_{ax} = 3.6m; the in-ward shifted configuration). This LHD configuration conforms the σ-optimized configuration and shows relatively good trapped particle orbit[4]. A significant performance of ICRF heating have also been demonstrated[5-8] and up to 500keV of energetic tail ions have been observed by fast neutral particle analysis (NPA)[9,10] in LHD.

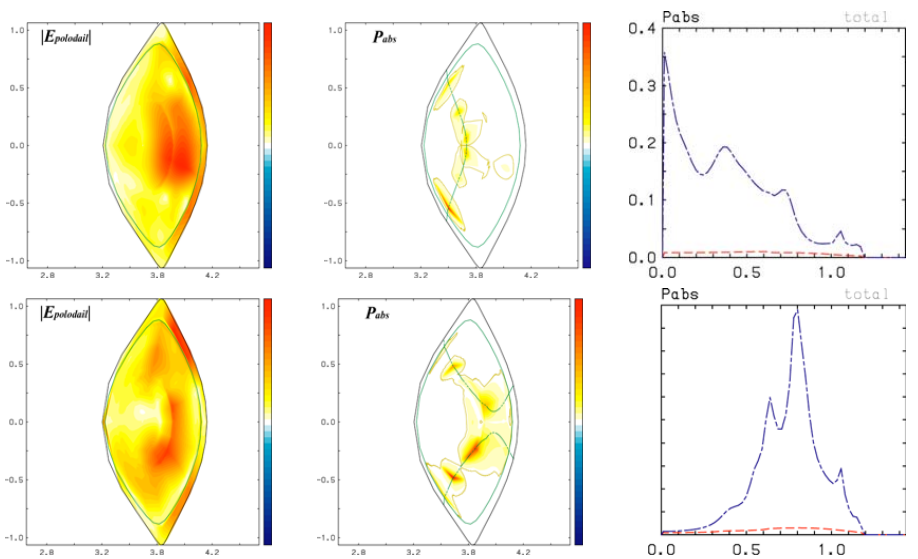

FIGURE 1. Contour plots of the poloidal electric field amplitude (left), RF power absorption (center) in the vertically elongated cross section, and the radial profile of power absorption (right) by TASK/WM code; the on-axis heating case (upper side) and the off-axis heating case (lower side).

The RF resonance position relative to magnetic flux surface has been tested mainly for two cases in the LHD experiments. One is the off-axis heating case in which the resonance surface almost crosses a saddle point of magnetic field at the longitudinally elongated cross section. In the off-axis case the resonance region only exists for $r/a>0.5$. The other is the on-axis heating in which the resonance surface crosses a magnetic axis. The experimentally obtained results have shown the difference in the heating efficiencies and about one order decrement of the energetic particle neutral count detected by natural diamond detector (NDD-NPA) [11].

We, first, applied the TASK/WM to the LHD plasmas in order to evaluate the RF wave electric fields (E_+ and E_-). Figure 1 shows the amplitude of the poloidal electric field (left) and power absorption (center) in the vertically elongated cross section, and the radial profile of the power absorption (right). The obtained results show the stronger RF wave field in the larger side of the major radius since the antenna is set in the outside of the torus.

From this result, a simple RF wave electric fields profile; $E_+ = E_{+0}\tanh((1-r/a)/l)\cos\theta$ with l=0.2 is assumed as a first step in the GNET simulation. The other wave field parameters are set as k_{perp}=62.8m^{-1} and $k_{//}$=0. The amplitude of the wave field, E_{+0}, is changed in the range 0.5kV/m through 1.5kV/m to obtain the dependency on the heating power. The plasma parameters are set to the similar values as the experimental ones. The plasma temperature and density are assumed as $T_s=T_{s0}(1-(r/a)^2)$ with $T_{e0}=T_{i0}$=1.6keV and $n_e=n_{e0}(1-(r/a)^8)$ with n_{e0}=1.0x10^{19}m^{-3}. We solve the drift kinetic equation for the proton minority ions distribution in the helium majority ions. The density ratio of the minority ion is assumed to be 5%.

Figure 2 shows the iso-surface plot of the steady state distribution of the minority ions during ICRF heating obtained by GNET. We plot the flux surface averaged tail ion distribution in the three dimensional space (r/a, E, θ_p), where a/r, E and θ_p are the normalized averaged minor radius, the total energy and the pitch angle, respectively.

The RF wave accelerates minority ions perpendicularly in the velocity space and we can see perpendicularly elongated minority ion distributions. We find a peaked energetic tail ion distribution near $r/a\sim0.5$ in the off-axis heating case (Fig.2, left). On the other hand we can see no strong peak in the distribution function in the on-axis heating case (Fig.2, left). The energetic particle distribution is broader than that of the off-axis case and the less energetic tail ion is obtained. A small peak can be seen very near the axis.

Figure 3 shows the radial profiles of the RF field power absorption and the energetic ion pressure of the minority ion. The absorption of the RF field shows the strong peak near r/a=0.5 in the off-axis case and near the axis in the on-axis case. The peaked pressure profile can be seen in the off axis case and the broader one is in the on-axis case. The higher peak observed in the distribution function of the off-axis case would be due to the stable orbit of the strongly absorbing trapped particles. We cannot see the strong peak due to the unstable orbit of those trapped particles in the on-axis case.

The heat deposition shows the maximum near *r/a*=0.5 in the off-axis case and flat one in the on axis case. The loss of the energetic tail ions actually alters the heating efficiency. The estimated heating efficiency (= the deposit power to the thermal plasma / the absorbed power of RF wave) changes up to about 2MW assuming 5% of minority ion density. The heating efficiencies with 1MW are about 70% for both cases and we can not see the clear difference between the two cases.

To compare with the experimental results we have simulated the neutral count number detected by NDD-NPA using the simulation results. Relatively good agreement is obtained between the experimental and simulation results (Fig.4). Both the computed and the experimental counts have similar dependency on the energy spectrum.

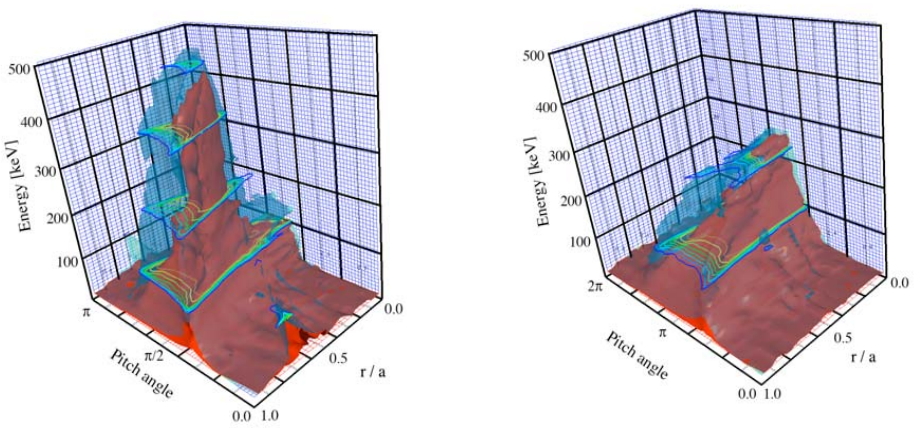

FIGURE 2. Steady state distribution of energetic tail ions in the (r/a, E, pitch angle) space in the off-axis point heating case (left) and on-axis heating case (right).

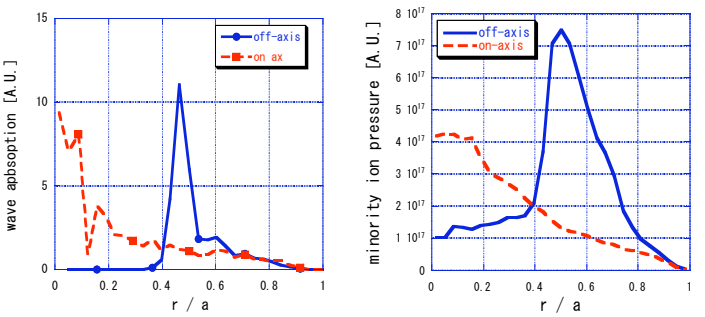

FIGURE 3. Radial profiles of ICRF wave power absorption (left) and energetic ion pressure (right) of the minority ion for the off-axis heating (solid) and the on-axis heating (dotted).

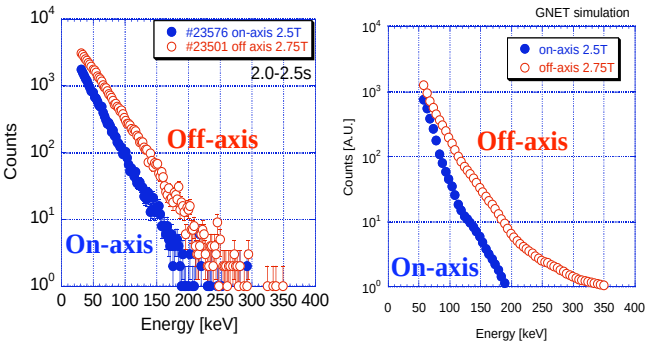

FIGURE 4. Comparisons of the energy spectrum by the NDD-NPA results (left) and the simulation results (right) for the off-axis heating (open) and the on-axis heating (closed).

SELF-CONSISTENT FULL WAVE ANALYSIS

Deviation of velocity distribution from Maxwellian may strongly affect the power absorption of ICRF waves in the presence of energetic ions, current drive efficiency of LHCD, NTM controllability of ECCD. In these cases a self-consistent analysis of wave propagation and absorption including the time evolution of the velocity distribution function and the local dielectric tensor is needed. We have implemented necessary interface code into the integrated modeling code system TASK [12] in order to study the case of ICRF minority heating.

The TASK code system has a modular structure and three modules are mainly related to the self-consistent full wave analysis. The full wave module (TASK/WM) solves Maxwell's equation with a local dielectric tensor calculated in the wave dispersion module (TASK/DP). The obtained wave electric field is used to calculate the bounce-averaged quasi-linear diffusion coefficients in the Fokker-Planck module (TASK/FP), which describes the time evolution of the velocity distribution function $f(v_{||},v_{\perp},t)$. Finally $f(v_{||},v_{\perp},t)$ is numerically integrated in velocity space to give the electric susceptibility for minority ions in TASK/DP. This loop has to be repeated until a quasi-steady state is obtained.

The module TASK/DP uses various kinds of plasma models to calculate the electric susceptibility for each particle species; cold plasma, kinetic plasma and gyrokinetic plasma models; Maxwellian and arbitrary velocity distribution functions; nonrelativistic and relativistic versions. For an arbitrary velocity distribution function $f(v_{||},v_{\perp},t)$, the calculation of susceptibility with the kinetic model requires numerical integration in velocity space

which consumes a lot of CPU time. If we calculate both the Hermite and anti-Hermite parts of the susceptibility, the computation time for 50 times 50 velocity-space meshes is about one thousand times longer than the time of usual calculation with the plasma dispersion function. Since the damping rate of the wave is essential, it may be worthwhile to compute only the anti-Hermite part of the susceptibility by numerical integration. In this case, the computation time is about one hundred times longer than that of usual calculation; one order of magnitude reduction compared with the computation including the Hermite part. Parallel processing will efficiently reduce the computation time. We also found that the accuracy of the Hermite part is much lower than that of the anti-Hermite part.

The module TASK/FP solves the bounce-averaged Fokker-Planck equation for the outer-mid-plane velocity distribution function $f(v_{||0}, v_{\perp 0}, t)$. In addition to the quasi-linear term, a nonlinear collision term, a parallel electric field term and a spatial diffusion term are included. The local distribution function $f(v_{||}, v_{\perp}, \theta, t)$ for any poloidal angle θ can be calculated from $f(v_{||0}, v_{\perp 0}, t)$.

The modules exchange the calculated data through the interface module TASK/PL; wave electric field (from WM to FP), local distribution function (from FP to DP), and dielectric tensor (from DP to WM). The universal data interface reduces the number of interface routines.

We have formulated and implemented the interface routines for self-consistent full wave analysis of the minority ion heating. Computation results will be reported very near future.

CONCLUSIONS

We have developed a global simulation code combining two code; GNET and TASK/WM. The GNET code solves a linearized drift kinetic equation for energetic ions including complicated behavior of trapped particles in 5-D phase space and the TASK/WM code solves Maxwell's equation for RF wave electric field with complex frequency as a boundary value problem in the 3D magnetic configuration. The developed code has been applied to the analysis of energetic tail ion transport during ICRF heating in the LHD plasma. A steady state distribution of energetic tail ion has been obtained and the characteristics of distribution in the phase space are clarified. The resonance position dependency on the distribution has been shown and larger tail formation has been obtained in the off-axis heating case. This tendency agrees well with the experimental results. We have compared the GNET simulation results with the experimental results evaluating NDD count number and also obtained similar tendencies.

Self-consistent analysis including the effect of energetic ion distribution on the fast wave propagation by TASK code is under way. Preliminary results of wave propagation and absorption with arbitrary velocity distribution function were discussed.

ACKNOWLEDGMENTS

This work was supported by Grant-in-Aid for Scientific Research from the Japanese Ministry of Education, Culture, Sports, Science and Technology.

REFERENCES

1. S. Murakami, et al, Nuclear Fusion **40** (2000) 693.
2. S. Murakami, et al., Fusion Sci. Technol. **46** (2004) 241.
3. A. Fukuyama, E. Yokota, T. Akutsu, Proc. 18th IAEA Conf. on Fusion Energy (Sorrento, Italy, 2000) **THP2-26**.
4. S. Murakami, et al., Nucl. Fusion **42** (2002) L19.
5. T. Mutoh, et al, Phys. Rev. Lett. **85** (2000) 4530.
6. R. Kumazawa, et al., Phys. Plasmas **8** (2001) 2139.
7. T. Watari, et al. Nucl. Fusion **41** (2001) 325.
8. T. Mutoh, et al., Fusion Sci. Technol. **46** (2004) 175.
9. A.V. Krashilnikov, et al., Nucl. Fusion 42 (2002) 759.
10. T. Saida, et al., Nuclear Fusion **44** (2004) 488.
11. M. Isobe, et al., Rev. Sci. Instrum. **72** (2001) 611.
12. A. Fukuyama, et al., Proc. of 20th IAEA Fusion Energy Conf. (Vilamoura, Portugal, 2004) IAEA-CSP-25/CD/TH/P2-3.